TECHNICAL PAPER

ISSN:1047-3289 *J. Air & Waste Manage. Assoc.* **57**:1326–1336
DOI:10.3155/1047-3289.57.11.1326

Revised Algorithm for Estimating Light Extinction from IMPROVE Particle Speciation Data

Marc Pitchford
National Oceanic and Atmospheric Administration, Las Vegas, NV

William Malm and Bret Schichtel
National Park Service, Fort Collins, CO

Naresh Kumar
Electric Power Research Institute, Palo Alto, CA

Douglas Lowenthal
Desert Research Institute, Reno, NV

Jenny Hand
Cooperative Institute Research in the Atmosphere, Colorado State University, Fort Collins, CO

ABSTRACT

The Interagency Monitoring of Protected Visual Environments (IMPROVE) particle monitoring network consists of approximately 160 sites at which fine particulate matter ($PM_{2.5}$) mass and major species concentrations and course particulate matter (PM_{10}) mass concentrations are determined by analysis of 24-hr duration sampling conducted on a 1-day-in-3 schedule. A simple algorithm to estimate light extinction from the measured species concentrations was incorporated in the 1999 Regional Haze Rule as the basis for the haze metric used to track haze trends. A revised algorithm was developed that is more consistent with the recent atmospheric aerosol literature and reduces bias for high and low light extinction extremes. The revised algorithm differs from the original algorithm in having a term for estimating sea salt light scattering from Cl^- ion data, using 1.8 instead of 1.4 for the mean ratio of organic mass to measured organic carbon, using site-specific Rayleigh scattering based on site elevation and mean temperature, employing a split component extinction efficiency associated with large and small size mode sulfate, nitrate and organic mass species, and adding a term for nitrogen dioxide (NO_2) absorption for sites with NO_2 concentration information. Light scattering estimates using the original and the revised algorithms are compared with nephelometer measurements at 21 IMPROVE monitoring sites. The revised algorithm reduces the underprediction of high haze periods and the overprediction of low haze periods compared with the performance of the original algorithm. This is most apparent at the hazier monitoring sites in the eastern United States. For each site, the PM_{10} composition for days selected as the best 20% and the worst 20% haze condition days are nearly identical regardless of whether the basis of selection was light scattering from the original or revised algorithms, or from nephelometer-measured light scattering.

IMPLICATIONS

Concerns raised about the use of the original IMPROVE algorithm for estimating light extinction from particle composition data for calculating the metric for tracking trends for the Regional Haze Rule (RHR) have been addressed in the formulation of a revised algorithm. The new algorithm reduces biases at the upper and lower extremes, which are of particular concern with regards to the RHR, which mandates reducing the impacts of manmade emissions on the 20% worst haze days while avoiding degradation of the 20% best haze conditions. The revised algorithm is likely to be adopted by most states for the technical assessments and modeling supporting their RHR state implementation plans.

INTRODUCTION

Atmospheric light extinction is a fundamental metric used to characterize air pollution impacts on visibility. It is the fractional loss of intensity in a light beam per unit distance due to scattering and absorption by the gases and particles in the air. Light extinction (b_{ext}) can be expressed as the sum of light scattering by particles ($b_{s,p}$), scattering by gases ($b_{s,g}$), absorption by particles ($b_{a,p}$) and absorption by gases ($b_{a,g}$). Traditionally, for visibility-protection applications, the most sensitive portion of the spectrum for human vision (550 nm) has been used to characterize light extinction and its components.

Light extinction due to the gaseous components of the atmosphere are relatively well understood and well estimated for any atmospheric conditions. Absorption of visible light by gases in the atmosphere is primarily by nitrogen dioxide (NO_2) and can be directly and accurately estimated from NO_2 concentrations by multiplying by the absorption efficiency. Scattering by gases is described

by the Rayleigh scattering theory. Rayleigh scattering depends on the density of the atmosphere, with the highest values at sea level (about 12 Mm^{-1}) and diminishing with elevation (8 Mm^{-1} at about 4 km), and varies somewhat at any elevation because of atmospheric temperature and pressure variations. Rayleigh scattering can be accurately determined for any elevation and meteorological conditions.

Particle light extinction is more complex than that caused by gaseous components. Light-absorbing carbon (e.g., diesel exhaust, soot, and smoke) and some crustal minerals are the only commonly occurring airborne particle components that absorb light. All particles scatter light, and generally particle light scattering is the largest of the four light extinction components. The amount of light scattered by an ensemble of particles can be quite accurately estimated using Mie theory when its size distribution and index of refraction are known.[1] Mie theory describes how electromagnetic energy (light as a function of wavelength) interacts with a particle as it passes through and around the particle. The scattering and absorption of the ensemble of particles is then calculated by summing over all particles with their various known optical and physical properties.[2] However, it is rare that the intrinsic optical and physical properties of each particle are known, so simplified calculation schemes are typically used to make extinction estimates.

The *I*nteragency *M*onitoring of *Pro*tected *V*isual *E*nvironments (IMPROVE) particle monitoring provides 24-hr duration mass concentrations for coarse (PM_{10}) and fine ($PM_{2.5}$) particulate matter (PM), as well as most of the $PM_{2.5}$ component concentrations on a 1-day-in-3 schedule. These data are routinely available at each of the approximately 160 IMPROVE monitoring sites for use in estimating light extinction. At 21 IMPROVE monitoring sites (Table 1), hourly averaged nephelometer and relative humidity (RH) data are also routinely available. Data from these sites have been key to evaluating the performance of the original IMPROVE algorithm, as well as for development and performance evaluation of various alternative revised algorithms.

Table 1. IMPROVE monitoring sites with nephelometers used to evaluate algorithm performance.

Abbreviation	Name	State	Region
ACAD	Acadia National Park	Maine	East
BIBE	Big Bend National Park	Texas	West
BOWA	Boundary Waters Canoe Area	Minnesota	East
CORI	Columbia River Gorge	Washington	West
DOSO	Dolly Sods/Otter Creek Wilderness	West Virginia	East
GICI	Gila Wilderness	New Mexico	West
GRCA	Grand Canyon National Park	Arizona	West
GRGU	Great Gulf Wilderness	New Hampshire	East
GRSM	Great Smoky Mountains	Tennessee	East
JARB	Jarbidge Wilderness	Nevada	West
LOPE	Lone Peak Wilderness	Utah	West
LYBR	Lye Brook Wilderness	Vermont	East
MACA	Mammoth Cave National Park	Kentucky	East
MORA	Mount Rainier National Park	Washington	West
MOZI	Mount Zirkel Wilderness	Colorado	West
OKEF	Okefenokee National Wildlife Refuge	Georgia	East
SHEN	Shenandoah National Park	Virginia	East
SHRO	Shining Rock Wilderness	North Carolina	East
SNAP	Snoqualamie Pass Wilderness	Washington	West
THIS	Three Sisters Wilderness	Oregon	West
UPBU	Upper Buffalo Wilderness	Arkansas	East

The IMPROVE algorithm for estimating light extinction was adopted by the U.S. Environmental Protection Agency (EPA) as the basis for the regional haze metric used to track progress in reducing haze levels for visibility-protected areas under the 1999 Regional Haze Rule (RHR).[3] As a result, the IMPROVE algorithm has been carefully scrutinized to assess deficiencies that could bias the implementation of the RHR.

The RHR uses the IMPROVE algorithm to estimate light extinction, which is then converted to the deciview haze index (i.e., a logarithmic transformation of b_{ext}). The RHR then calls for the determination of the mean of the annual 20% best and 20% worst haze days for each of the IMPROVE monitoring sites that represent the visibility-protected areas. States are asked to manage emissions so that over a 60-yr period the worst haze days will improve to natural conditions without degrading visibility conditions for the best haze days. For consistency, the same approach (i.e., IMPROVE algorithm and conversion to the deciview haze index) is also used to estimate natural haze levels for each representative monitoring site using estimates of the natural concentration levels for the major particle components. For each location, the linear rate of reduction of the deciview values for the worst haze days during the baseline period (2000–2004) that is needed to reach the estimated worst haze days under natural conditions by 2064 must be determined. This linear rate is used as a guide to pace the desired rate of haze reduction and to determine interim visibility goals that are compared to the monitoring data trends of the best and worst haze days.

The RHR emphasizes the extremes of light extinction through its requirement to estimate best and worst haze days for the baseline period and for estimates of natural worst haze conditions. Also, the use of the deciview index means that additive biases in the light extinction estimates (e.g., the use of a standard Rayleigh scattering term for all sites regardless of elevation) will affect the calculation of a linear glide slope, which is a guide used to set the pace of emission reductions. Use of the IMPROVE algorithm for the RHR elicited concerns about possible biases in the apportionment among the various major particle components. Such issues have been the subject of a number of critical reviews of the use of the IMPROVE algorithm in the RHR.[4,5]

In light of the concerns raised by its use in the RHR, the IMPROVE Steering Committee initiated an internal review, including recommendations for revisions of the IMPROVE algorithm for estimating light extinction. The full report of this review is available elsewhere.[6] Subsequently, the IMPROVE Steering Committee established a subcommittee to develop a revised algorithm that reduces biases in light extinction estimates and is as consistent as possible with the current scientific literature, while constrained by the need to use only those data that are routinely available from the IMPROVE particle monitoring network. The resulting algorithm was accepted for use by the IMPROVE Steering Committee and is being used by

most states in their implementation of the RHR. The primary purpose of this paper is to describe the revised algorithm, summarize the rationale for each of the changes from the original algorithm, and characterize the performance of the original and revised algorithms.

Original IMPROVE Algorithm

The original IMPROVE algorithm for estimating light extinction from IMPROVE particle monitoring data assumes that absorption by gases ($b_{a,g}$) is zero, that Rayleigh scattering ($b_{s,g}$) is 10 Mm^{-1} for each monitoring site regardless of site elevation and meteorological condition, and that particle scattering and absorption ($b_{s,p}$ and $b_{a,p}$) can be estimated by multiplying the concentrations of each of six major components by typical component-specific mass extinction efficiencies. The six major components are sulfate (assumed to be ammonium sulfate), nitrate (assumed to be ammonium nitrate), organic compounds (based on measured organic carbon [OC] mass), elemental or black carbon (directly measured), fine soil (crustal elements plus oxides) and coarse mass (the difference between PM_{10} and $PM_{2.5}$ mass concentrations). The component dry mass extinction efficiency values are expressed as single significant digit constants, reflecting the level of uncertainty of these values. The sulfate and nitrate mass extinction efficiency terms include a water growth factor that is a function of RH (displayed as *f(RH)*) multiplied by a constant dry extinction efficiency. Monthly averaged water growth terms for each site were developed because most monitoring sites do not include on-site RH monitoring. Expressed as an equation, the original algorithm for estimating light extinction from IMPROVE data takes the following form where the particle component concentrations are indicated in the brackets. The formulas for the composite components are available elsewhere.[7]

$$\begin{aligned} b_{ext} \approx\ & 3 \times f(RH) \times [Sulfate] + 3 \times f(RH) \times [Nitrate] \\ & + 4 \times [Organic\ Mass] \\ & + 10 \times [Elemental\ Carbon] \\ & + 1 \times [Fine\ Soil] + 0.6 \times [Coarse\ Mass] \\ & + 10 \end{aligned} \quad (1)$$

The units for light extinction and Rayleigh scattering are inverse megameters ($1/10^6$ m usually written Mm^{-1}); component concentrations shown in brackets are in microgram per meter cubed ($\mu g/m^3$); dry mass extinction efficiency terms are in units of meters squared per gram (m^2/g); and the water growth terms, *f(RH)*, are unitless.

Among the implicit assumptions for this formulation of the algorithm are that

- Six particle component terms plus a constant Rayleigh scattering term are sufficient for a good estimate of light extinction;
- Constant dry mass extinction efficiency terms rounded to one significant digit for each of the six particle components (e.g., for both sulfate and nitrate the value is 3) works adequately for all locations and times; and
- Light extinction contributed by the individual particle components can be adequately estimated as separate terms as they would if they were in completely separate particles (externally mixed), though they often are known to be internally mixed in particles.

A relatively simple algorithm for estimating light extinction using only the available monitoring data requires assumptions such as these.

Estimates of particle scattering by this algorithm (i.e. excluding the light absorbing carbon and Rayleigh terms) have been compared with directly measured particle scattering data at the 21 monitoring sites that have hourly averaged nephelometer and RH data. As shown in Figure 1, the algorithm performs reasonably well over a broad range of particle light scattering values and monitoring locations. The algorithm tends to underestimate the highest extinction values and to overestimate the lowest extinction values. Since its first use,[7] the original algorithm has been a useful tool that significantly contributed to a better understanding of haze levels and the relative magnitude of haze contribution by the various particle components.

Revised IMPROVE Algorithm

A revised algorithm was developed to address issues raised concerning the original algorithm. The revised algorithm meets many of the overall design criteria of the original,

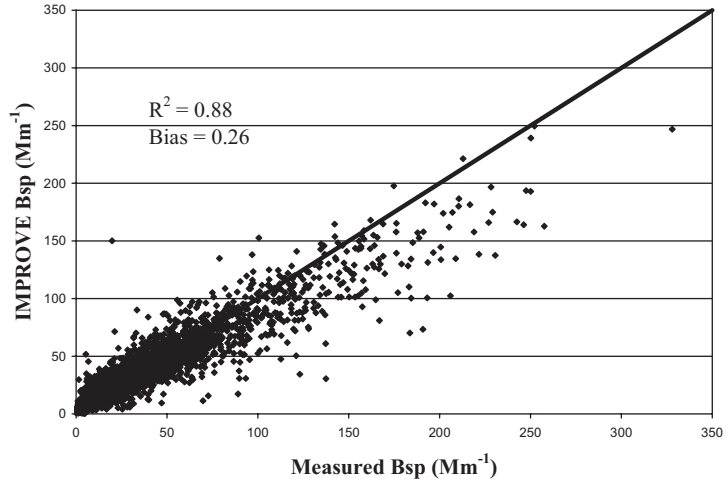

Figure 1. A scatter plot of the original IMPROVE algorithm estimated particle light scattering vs. measured particle light scattering.

including that it is a relatively simple algorithm that produces consistent estimates of light extinction for all remote-area IMPROVE aerosol monitoring sites and permits the individual particle component contributions to light extinction to be separately estimated. Five major revisions were made to the original IMPROVE algorithm for estimating light extinction from IMPROVE particle speciation data. They include

- Addition of a sea salt term, which is a particular concern for coastal monitoring locations in which the sum of the major components of light extinction and mass has been deficient;
- Change of the assumed organic compound mass to OC mass ratio from 1.4 to 1.8 to reflect more recent peer-reviewed literature on the subject;
- Use of site-specific Rayleigh scattering based on the elevation and annual average temperature of the monitoring sites;
- Development and use of a split component extinction efficiency model for sulfate, nitrate, and OC components, including new water growth terms for sulfate and nitrate to better estimate light extinction at the high and low extremes of the range; and
- Addition of a NO_2 light absorption term that would only be used at sites with available NO_2 concentration data.

The technical rationale for making each of these changes is described in separate sections below.

Sea Salt

The original IMPROVE protocol for estimating light extinction does not include light scattering (b_{sp}) by sea salt aerosols. Lowenthal and Kumar[4] demonstrated that inclusion of elements from sea salt (e.g., sodium [Na], chlorine [Cl]) increased the accuracy of mass reconstruction at coastal IMPROVE sites. Contributions of sea salt particles to light extinction at some coastal IMPROVE sites may be significant, especially because b_{sp} by sea salt particles should be significantly enhanced by hygroscopic growth in humid environments. Lowenthal and Kumar[8] found that fine sea salt aerosols accounted for 43% of estimated b_{sp} at the U.S. Virgin Islands IMPROVE site. Coastal area sea salt is a natural source of haze that will increase in relative importance as anthropogenic contributions are reduced.

To include sea salt in the IMPROVE light extinction equation, it is necessary to: (1) estimate the sea salt mass concentration; (2) specify a dry sea salt mass scattering efficiency; and (3) specify an *f(RH)* curve for sea salt representing the enhancement of sea salt scattering by hygroscopic growth as a function of RH.

Sea Salt Mass Concentration. Estimating sea salt mass requires a sea salt marker species measured in IMPROVE aerosol samples. The most obvious markers are Na and Cl, because NaCl is the main component in seawater and sea salt. Based on the composition of sea water, pure sea salt mass is Na multiplied by 3.1 or Cl multiplied by 1.8.[9] However, Na is poorly quantified by the X-ray fluorescence (XRF) used by IMPROVE and Cl can be depleted in ambient aerosol samples by acid-base reactions between sea salt particles and sulfuric and nitric acids.[10] Without accurate measurement of both Na (or other conservative tracers) and Cl, it is not possible to estimate how much Cl has been replaced by nitrate and/or sulfate in ambient samples. Further, without chemical speciation of the PM_{10} sample (Module D of the IMPROVE sampler), it is not possible to estimate coarse sea salt scattering.

Given these limitations, the revised algorithm estimates the $PM_{2.5}$ sea salt concentration as the concentration of chloride ion (Cl^-) measured by ion chromatography multiplied by 1.8. If the chloride measurement is below the detection limit, missing, or invalid, then the $PM_{2.5}$ sea salt concentration should be estimated as the concentration of Cl measured by XRF multiplied by 1.8.

Although the XRF measurement can detect Cl at lower concentrations, the A-module sample for XRF is more exposed to reactive losses because acidic gases are not removed from the airstream and any HCl they release from the sample is not retained by the Teflon filter. Unless speciated data become available for PM_{10}, coarse sea salt mass and light scattering will not be considered. To the degree that Cl^- has been replaced by sulfate or nitrate in ambient particles, this approach will underestimate the mass and scattering contributed by the substituted sea salt that results (e.g. $NaNO_3$, $NaHSO_4$, or Na_2SO_4). This mass is partially accounted for by ammonium sulfate and ammonium nitrate in the IMPROVE equation. However, the substituted Na salt mass is underestimated because ammonium is lighter than sodium. The scattering is also underestimated because the sodium salts absorb more water than does ammonium sulfate above 60% RH. On the other hand, the 1.8 factor accounts for sea salt constituents such as calcium (Ca) and magnesium (Mg), which are included in the fine soil aerosol composite component, resulting in a small double counting of mass. Given the limitations of the available data, 1.8 times Cl^- provides a reasonable and likely lower-limit to the fine sea salt mass.

Sea Salt Dry Mass Scattering Efficiency. To estimate the dry mass scattering efficiency and *f(RH)* for sea salt aerosols, their dry mass size distribution must be known. Although this has not been measured at most IMPROVE sites, extensive sea salt size distribution measurements have been made in the remote marine environment during cruise-based experiments.[11–13] On the basis of these studies, a dry log-normal mass size distribution with a geometric mean diameter (D_g) of 2.5 μm and geometric standard deviation (σ_g) of 2 is recommended. A dry scattering efficiency for $PM_{2.5}$ sea salt of 1.7 m^2/g was calculated using the Mie theory on the basis of this size distribution assuming a sea salt refractive index of [1.55+ i0] and a density of 1.9 $g \cdot cm^{-3}$ recommended by Quinn et al.[11]

Sea Salt f(RH). Tang et al.[14] determined hygroscopic growth curves for aerosols generated from Long Island, NY, and Atlantic Ocean seawater. The water absorption curves for sea salt were nearly identical to that of NaCl. The NaCl growth factors derived from the AIM3 thermodynamic equilibrium model[15] are shown in Table 2 as a function of RH. Below the crystallization point (RH = 47%), the growth factor is set to 1. Values are presented to

Table 2. Sea salt particle diameter growth and water growth function.

RH (%)	Growth Factor[a]	*f(RH)*	RH (%)	Growth Factor	*f(RH)*
1–46	1.0000	1.0000	71	1.8434	3.1269
47	1.5922	2.3584	72	1.8589	3.1729
48	1.6001	2.3799	73	1.8751	3.2055
49	1.6081	2.4204	74	1.8921	3.2459
50	1.6162	2.4488	75	1.9100	3.2673
51	1.6245	2.4848	76	1.9288	3.3478
52	1.6329	2.5006	77	1.9488	3.4174
53	1.6415	2.5052	78	1.9700	3.5202
54	1.6503	2.5279	79	1.9925	3.5744
55	1.6593	2.5614	80	2.0166	3.6329
56	1.6685	2.5848	81	2.0423	3.6905
57	1.6779	2.5888	82	2.0701	3.8080
58	1.6875	2.6160	83	2.1001	3.9505
59	1.6974	2.6581	84	2.1328	4.0398
60	1.7075	2.6866	85	2.1684	4.1127
61	1.7179	2.7341	86	2.2077	4.2824
62	1.7286	2.7834	87	2.2512	4.4940
63	1.7397	2.8272	88	2.2999	4.6078
64	1.7511	2.8287	89	2.3548	4.8573
65	1.7629	2.8594	90	2.4174	5.1165
66	1.7751	2.8943	91	2.4898	5.3844
67	1.7877	2.9105	92	2.5749	5.7457
68	1.8008	2.9451	93	2.6769	6.1704
69	1.8145	3.0105	94	2.8021	6.7178
70	1.8286	3.0485	95	2.9610	7.3492

Notes: [a]Diameter at RH/dry diameter.

RH = 95%, to which higher RH are "rolled back" under the RHR protocol[3] to mitigate the potentially large errors associated with RH measurement uncertainty for near saturation conditions. Dry (RH = 0%) light scattering ($b_{sp(Dry)}$) was calculated using Mie theory for sea salt at unit $PM_{2.5}$ mass concentration with the dry mass size distribution, refractive index, and density described above. Light scattering at RH = 46–95% at unit RH intervals ($b_{sp(RH)}$) was calculated by applying the NaCl growth curve (Table 2) to the dry mass size distribution using Mie theory, accounting for the change in particle volume and refractive index from the addition of water. The *f(RH)* values, defined as $b_{sp(RH)}/b_{sp(Dry)}$, are listed in Table 2. The *f(RH)* values in Table 2 were used to generate monthly, site-specific "climatological" values using long-term hourly RH data representative of each of the IMPROVE monitoring sites, as was done in the original algorithm for ammonium sulfate/ammonium nitrate. Light scattering by sea salt (SS) aerosols is estimated as indicated in eq 2.

$$b_{sp(SS)} = 1.7 f_{SS}(RH)[1.8 * Cl^-] \quad (2)$$

Organic Mass to Organic Carbon Ratio

For the original IMPROVE algorithm, a factor of 1.4 was used to convert OC to organic mass (OM) to account for unmeasured elements (e.g. O, H, N) in OM. The value of 1.4 was based on an experiment conducted by Grosjean and Friedlander[16] in urban Pasadena, CA, in 1973. They found that the carbon content of these samples averaged 73%. White and Roberts[17] suggested an OC to OM conversion factor (OM/OC) of 1.4, the reciprocal of 0.73. Andrews et al.[18] attempted to explain the reconstructed mass deficit during SEAVS (Southeastern Aerosol and Visibility Study) at the Great Smoky Mountains National Park in terms of underestimation of OM.

Turpin and Lim[19] recommended the use of OM/OC factors of 1.6 ± 0.2 and 2.1 ± 0.2 for urban and nonurban aerosol, respectively, based on the chemical structure of organic compounds found in such environments. This is consistent with an expectation that the OM/OC ratio should increase as aerosols age during transport and photochemical reactions produce secondary organic compounds that are more oxygenated than their primary precursors. Krivácsy et al.[20] isolated the polar, water-soluble OC fraction of aerosols from the Jungfraujoch, Switzerland using solid phase extraction. An OM/OC ratio of 1.91 was inferred from elemental composition (C, N, H, and S). Poirot and Husar[21] found that agreement between reconstructed and measured $PM_{2.5}$ was closer with an OM/OC ratio of 1.8 than with the factor of 1.4 for samples from the IMPROVE and STN networks in the northeastern United States during summer 2002, when large impacts from forest fires in Quebec were observed. Malm et al.[22] found that $PM_{2.5}$ mass and light scattering closure was achieved assuming an OM/OC ratio of 1.8 during a two-month study at Yosemite National Park in summer 2002. El-Zanan et al.[23] derived OM/OC ratios of 1.92 ± 0.40 from solvent extracts of archived filter samples from five IMPROVE sites and 2.07 ± 0.32 from chemical mass balance in 40,532 daily IMPROVE samples at 50 sites from 1988–2003. Malm and Hand[24] estimated OM/OC ratios at 160 IMPROVE monitoring sites using regression analysis and found an average across all sites of 1.7 ± 2.4, with the highest values (>1.9) generally for sites in the west and that are often influenced by biogenic smoke and the lowest values (~1.4) for sites in the central and northeastern United States and in urban areas.

Although additional experimental work is needed to further explore this issue, it is clear that an OC conversion factor of 1.4 is not generally applicable for remote areas of the United States. On the basis of the recent research, a value of 1.8 was selected for use in the revised algorithm as more applicable for remote area datasets.

Split Component Mass Extinction Efficiency Model

Concentration-Varying Dry Mass Scattering Efficiencies. The original IMPROVE algorithm employs dry mass scattering efficiencies of 3 m^2/g for ammonium sulfate and ammonium nitrate and 4 m^2/g for OM. Data from IMPROVE special studies suggest that dry mass extinction efficiencies are variable. Lowenthal and Kumar[25] found that $PM_{2.5}$ mass scattering efficiencies increased with increasing levels of particle light scattering and mass concentration. This was attributed to growth of the dry particle size distribution into size ranges with higher scattering efficiencies under more-polluted conditions, which are related to a higher degree of cloud processing during transport. Malm et al.[26] estimated dry ammoniated sulfate mass scattering efficiencies ranging from 2.4–4.1 m^2/g during the Big Bend Aerosol and Visibility Observational Study (BRAVO). A weak relationship between efficiency

and ammoniated sulfate mass concentration was reported. Malm and Hand[24] using regression analysis found that organic and inorganic fine mass dry mass scattering efficiencies have a functional dependence on mass concentration at most of the 21 sites with collocated IMPROVE aerosol and nephelometer measurements.

The revised IMPROVE algorithm accounts for the increase of ammonium sulfate/ammonium nitrate and OM efficiencies with concentration using a simple mixing model in which the concentrations of ammonium sulfate, ammonium nitrate, and OM are each comprised of external mixtures of mass in small and large particle size modes. The large mode represents aged and/or cloud processed particles, whereas the small mode represents freshly formed particles. These size modes are described by log-normal mass size distributions with D_g and geometric standard deviations (σ_g) of 0.2 μm and 2.2 for small mode and 0.5 μm and 1.5 for the large mode, respectively. The dry mass $PM_{2.5}$ scattering efficiencies for small- and large-mode ammonium sulfate (2.2 and 4.8 m^2/g), ammonium nitrate (2.4 and 5.1 m^2/g), and OM (2.8 and 6.1 m^2/g) were calculated using the Mie theory at a wavelength of 550 nm based on the log-normal mass size distribution parameters described above. The ammonium sulfate, ammonium nitrate, and OM densities and refractive indexes used in this calculation are 1.77, 1.73, and 1.4 g/cm^3, respectively, and 1.53 + i0, 1.55 + i0, and 1.55 + i0, respectively. No attempt was made to account for possible difference in composition between the two size modes of these particles.

Use of the split component approach requires a method to estimate the apportionment of the total fine particle concentration of each of the three measured species into the concentrations of the small and large size fractions. The selected method was empirically developed and evaluated using the light scattering and composition data for the 21 monitoring sites with nephelometer data (Table 1). The fraction of the fine particle component (sulfate, nitrate, or organic mass) that is in the large mode is estimated by dividing the total concentration of the component by 20 $\mu g/m^3$ (e.g., if the total fine particulate OC concentration is 4 $\mu g/m^3$, the large mode concentration is calculated to be one-fifth of 4 $\mu g/m^3$ or 0.8 $\mu g/m^3$, leaving 3.2 $\mu g/m^3$ in the small mode). If the total concentration of a component exceeds 20 $\mu g/m^3$, all of it is assumed to be in the large mode. Alternate values were tested for the 20-$\mu g/m^3$ value used in this empirical approach, including use of species-specific values designed to improve the performance in estimating light scattering. The modest performance improvements associated with the best of these alternate values was not considered sufficient justification for trying to further tune these values to fit the available light scattering dataset.

f(RH). The original IMPROVE algorithm applies a single *f(RH)* curve to ammonium sulfate and ammonium nitrate scattering, which is based on a hygroscopic growth curve [$D_{(RH)}/D_{(Dry)}$, the particle diameter at ambient RH divided by the dry particle diameter] for pure ammonium sulfate that was smoothed between the deliquescence and efflorescence branches.[3] The revised IMPROVE algorithm contains *f(RH)* curves for small- and large-mode ammonium sulfate that are also applied to small and large mode ammonium nitrate. The *f(RH)* for OM is assumed to be 1 at all RH for small and large OM modes. This assumption is based principally on a lack of evidence for water growth by ambient particulate OM. Additional experimental work is needed to further explore this issue. The *f(RH)* for ammonium sulfate and ammonium nitrate are based on the hygroscopic growth curve for pure ammonium sulfate derived from the AIM thermodynamic equilibrium model.[15] This growth curve represents the upper branch, also referred to as the efflorescence or hysteresis branch, of the ammonium sulfate growth curve. The upper branch is

Table 3. Water growth for the small and large sized distribution sulfate and nitrate components.

RH (%)	$f_S(RH)$	$f_L(RH)$	RH (%)	$f_S(RH)$	$f_L(RH)$	RH (%)	$f_S(RH)$	$f_L(RH)$
0–36	1.00	1.00	56	1.78	1.61	76	2.60	2.18
37	1.38	1.31	57	1.81	1.63	77	2.67	2.22
38	1.40	1.32	58	1.83	1.65	78	2.75	2.27
39	1.42	1.34	59	1.86	1.67	79	2.84	2.33
40	1.44	1.35	60	1.89	1.69	80	2.93	2.39
41	1.46	1.36	61	1.92	1.71	81	3.03	2.45
42	1.48	1.38	62	1.95	1.73	82	3.15	2.52
43	1.49	1.39	63	1.99	1.75	83	3.27	2.60
44	1.51	1.41	64	2.02	1.78	84	3.42	2.69
45	1.53	1.42	65	2.06	1.80	85	3.58	2.79
46	1.55	1.44	66	2.09	1.83	86	3.76	2.90
47	1.57	1.45	67	2.13	1.86	87	3.98	3.02
48	1.59	1.47	68	2.17	1.89	88	4.23	3.16
49	1.62	1.49	69	2.22	1.92	89	4.53	3.33
50	1.64	1.50	70	2.26	1.95	90	4.90	3.53
51	1.66	1.52	71	2.31	1.98	91	5.35	3.77
52	1.68	1.54	72	2.36	2.01	92	5.93	4.06
53	1.71	1.55	73	2.41	2.05	93	6.71	4.43
54	1.73	1.57	74	2.47	2.09	94	7.78	4.92
55	1.76	1.59	75	2.54	2.13	95	9.34	5.57

used because deliquescence is rarely observed in the environment. Because pure ammonium sulfate crystallizes at 37% RH, it is assumed that there is no hygroscopic growth and that the *f(RH)* is one below this RH.

Dry (RH = 0%) light scattering ($b_{sp(Dry)}$) was calculated using Mie theory for small- and large-mode ammonium sulfate. Light scattering at RH = 37–95% at unit RH intervals ($b_{sp(RH)}$) was calculated by applying the AIM ammonium sulfate growth curve to the small and large dry mode size distributions using Mie theory, accounting for the change in particle volume and refractive index from the addition of water. The *f(RH)*, defined as $b_{sp(RH)}/b_{sp(Dry)}$, are listed in Table 3 for the small ($f_{(S)}RH$) and large ($f_{(L)}RH$) modes. Values are presented to RH = 95%, to which higher RH are "rolled back" under the RHR protocol.[3] The same *f(RH)* are applied to small- and large-mode ammonium sulfate and ammonium nitrate.

Site-Specific Rayleigh Scattering

Rayleigh scattering refers to the scattering of light from the molecules of the air, and a constant value of 10 Mm^{-1} is used in the original IMPROVE algorithm. However, Rayleigh scattering depends on the density of the air and thus varies with temperature and pressure. Site-specific Rayleigh scattering was estimated using a Rayleigh Scattering Calculator developed by Air Resource Specialists, Inc. that calculates Rayleigh scattering as a function of temperature and pressure. For each IMPROVE site, we used the standard U.S. atmospheric pressure corresponding to the monitoring site elevation, and an estimated annual mean temperature. The temperature data were obtained from the nearest weather stations for time periods encompassing 10–30 yr and were interpolated to the monitoring site location. Site-specific Rayleigh scattering calculated using this procedure is available for each IMPROVE monitoring site on the IMPROVE and VIEWS Web sites.[27] These are integer-rounded, site-specific values that range from 8 Mm^{-1} for sites at about 4 km elevation to 12 Mm^{-1} for sites near sea level.

NO_2 Absorption

An NO_2 absorption efficiency term (PAE_{NO2}) was calculated by dividing the sum of the products of the relative observer photopic response values, PR(λ), for viewing an image of 2° angular size and the spectral NO_2 absorption efficiency values, AE(λ), by the sum of the photopic response values over the wavelength range of 350–755 nm, as shown in eq 3.

$$PAE_{NO_2} = \frac{\sum_{350}^{750} PR(\lambda) \times AE(\lambda)}{\sum_{350}^{750} PR(\lambda)} \quad (3)$$

The spectral NO_2 absorption efficiency values are from Dixon[28] and available in the PLUVUE Users Manual,[29] where they were given in 10-ηm increments that were interpolated to generate 1-ηm values. The PR values are from the CIE Ybar function downloaded directly from the CVRL Color and Vision database.[30] Both curves are shown in Figure 2. The resulting photopic-weighted absorption efficiency value (PAE_{NO2}) equals 0.33 Mm^{-1}/ppb.

A lack of NO_2 monitoring data at IMPROVE sites limits the utility of the NO_2 light absorption term in the revised algorithm. It was included for completeness should any of the sites initiate such monitoring, and to allow model-estimated NO_2 concentrations to be, incorporated into an estimated light extinction calculation. For

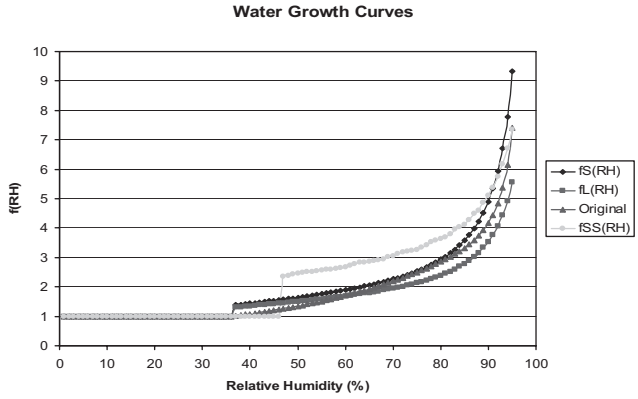

Figure 3. Water growth curves for small and large size distribution sulfate and nitrate, sea salt, and the original IMPROVE algorithm sulfate and nitrate.

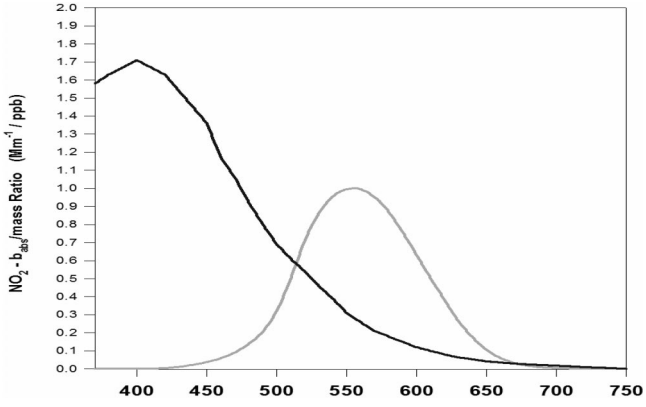

Figure 2. NO_2 absorption coefficient and 2° observer PR curves as a function of wavelength (ηm).

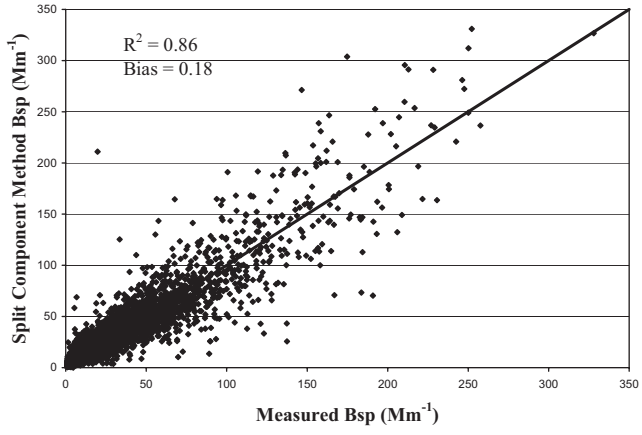

Figure 4. Scatter plot of the revised algorithm estimates of light scattering vs. measured light scattering.

Table 4. Average fractional bias by quintiles for the original and revised algorithms for sites east and west of the 100th meridian.

	Quintile 1		Quintile 2		Quintile 3		Quintile 4		Quintile 5	
Region	**Original**	**Revised**	**Original**	**Revised**	**Original**	**Revised**	**Original**	**Revised**	**Original**	**Revised**
East	0.63	0.47	0.24	0.14	0.15	0.09	0.06	0.06	−0.11	−0.01
West	1.04	0.81	0.35	0.23	0.17	0.07	0.07	0.01	−0.08	−0.10

remote areas, the relative NO_2 contributions to light extinction are generally considered too small to justify their assessment. However, the NO_2 concentrations in plumes and layers near sources with good particle emission controls could make significant contributions to the total light extinction and produce a noticeable brown appearance to the plume or layer.

Revised Algorithm

The revised algorithm is shown in eq 4, with the new and changed terms printed in boldface to emphasize the difference from the original IMPROVE algorithm.

$$\begin{aligned} b_{ext} \approx\ & \mathbf{2.2 \times f_S(RH) \times [Small\ Sulfate]} \\ & \mathbf{+ 4.8 \times f_L(RH) \times [Large\ Sulfate]} \\ & \mathbf{+ 2.4 \times f_S(RH) \times [Small\ Nitrate]} \\ & \mathbf{+ 5.1 \times f_L(RH) \times [Large\ Nitrate]} \\ & \mathbf{+ 2.8 \times [Small\ Organic\ Mass]} \\ & \mathbf{+ 6.1 \times [Large\ Organic\ Mass]} \\ & + 10 \times [Elemental\ Carbon] + 1 \times [Fine\ Soil] \\ & \mathbf{+ 1.7 \times f_{SS}(RH) \times [Sea\ Salt]} \\ & + 0.6 \times [Coarse\ Mass] \\ & \mathbf{+ Rayleigh\ Scattering\ (Site\ Specific)} \\ & \mathbf{+ 0.33 \times [NO_2\ (ppb)]} \end{aligned} \quad (4)$$

Comparing this to the original algorithm (eq 1), notice that the three split components (i.e. sulfate, nitrate, and organic mass) have dry mass extinction efficiencies that are smaller than the original dry mass extinction efficiency values for the small particle size modes and larger than the original values for the large particle size modes. This permits the new algorithm to perform better than the original algorithm with its single dry mass extinction efficiency at the concentration extremes where either the small or large particle size modes will dominate, resulting in less or more efficient particle light scattering.

The water growth curves for the large and small particle size modes for sulfate and nitrate, and for sea salt are shown in Figure 3 along with the water growth curve used in the original algorithm for sulfate and nitrate. The large and small particle size mode growth curves exceed the original algorithm growth curve for RH less than approximately 60% because the original growth curve was estimated to be an average of the upper and lower hysteresis branches of the ammonium sulfate curve, whereas the curves used for the revised algorithm are solely the upper branch of the ammonium sulfate curve. At higher RH, the large particle size mode *f(RH)* is below the original curve, whereas the small particle size mode *f(RH)* is above the original curve.

Algorithm Performance Evaluation

Performance of the original and revised algorithm for estimating extinction can be assessed in a number of ways each of which serves to answer different questions. Reduction of the biases in light scattering estimates at the extremes (i.e. underestimation of the high values and overestimation of the low values) when compared with nephelometer measurements was one of the most compelling reasons for development of a new algorithm, so comparisons of bias for the original and revised algorithm are one way to evaluate performance.

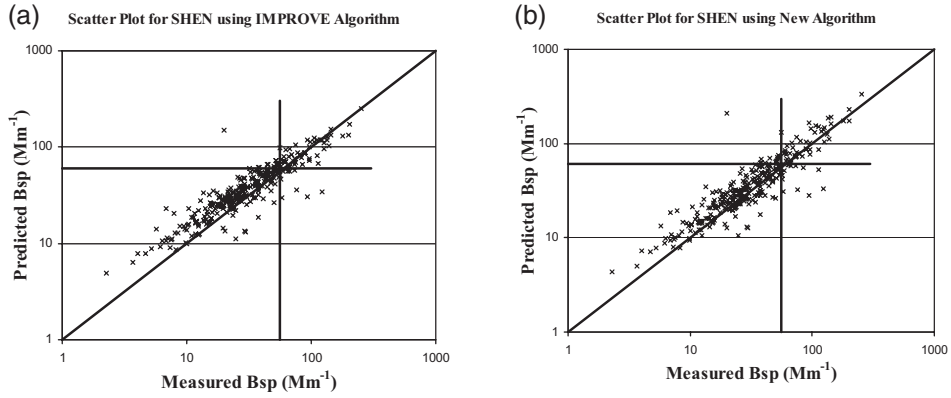

Figure 5. Scatter plots of the (a) original IMPROVE and (b) revised algorithm estimates of light scattering vs. measured light scattering for Shenandoah National Park. Horizontal and vertical lines are at the 80th percentile for estimated and measured light scattering.

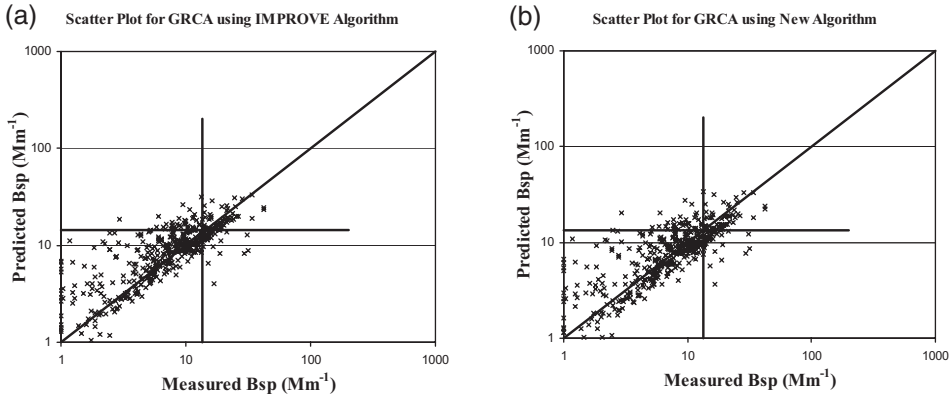

Figure 6. Scatter plots of the (a) original IMPROVE and (b) revised algorithm estimates of light scattering vs. measured light scattering for Grand Canyon National Park. Horizontal and vertical lines are at the 80th percentile for estimated and measured light scattering.

Scatter plots of light scattering estimates from the original and new proposed algorithms versus nephelometer data (Figures 1 and 4, respectively) for all available data at 21 monitoring sites are one way to view the overall performance differences between the two algorithms. These figures show that the bias at the extremes is reduced using the new algorithm (bias = 0.18) compared with the original IMPROVE algorithm (bias = 0.26) (i.e., the points tend to be better centered on the one-to-one line). They also show that the new algorithm has marginally greater uncertainty (r^2 = 0.86) compared with the original algorithm (r^2 = 0.88). Although these plots are weighted toward sites with longer sample histories, it is also the case that the average fractional bias is lower at 19 of the 21 sites. The averages of the site-averaged fractional biases are 0.25 and 0.17 for the original and revised algorithms, respectively. Table 4 shows the averaged fractional bias in quintiles of measured particle light scattering by region of the country in which the 21 monitoring sites are located (as shown in Table 1, East includes the 11 sites east of the one-hundredth meridian and West includes the 10 remaining sites). The bias values for the original algorithm are reduced for the revised algorithm for most of the quintiles in both East and West regions.

Figures 5 and 6 are scatter plots for two individual sites, Shenandoah and Grand Canyon National Parks. The logarithmic scales on these plots exaggerate the scatter for low values compared with high values. The individual-site scatter plots have the 80th percentile values indicated on the graphs for the predicted and measured values by horizontal and vertical lines respectively. Points that are to the right of the vertical line have nephelometer values that are among the 20% worst light scattering for that monitoring site. Points that are above the horizontal line have algorithm-determined values that are among the 20% worst estimated light scattering for that monitoring site.

The revised algorithm performs better with respect to having data points more centered on the one-to-one line at the high and low haze level extremes (bias = 0.04 and 0.40, respectively) than the original IMPROVE algorithm (bias = −0.04 and 0.55, respectively) for Shenandoah National Park, which is typical for the high haze level locations in the southeast United States A large number of the measured worst haze sample periods are correctly identified by the original (81%) and revised (76%) algorithms (these are the points above and to the right of the two 80th percentile lines). The differences between the two algorithms for Grand Canyon National Park and most of the other much less hazy locations are not as apparent in these scatter plots.

Table 5 shows the performance of the original and revised algorithms in correctly classifying sample periods into the 20% best and the 20% worst visibility days on the basis of nephelometer measurements for the East and West regions. Although the results are similar between the two algorithms, the modestly greater extinction estimation uncertainty for the revised algorithm results in its misclassification of 1–3% more sample periods than the original algorithm. To evaluate the significance of the misclassification by either algorithm, the average composition of the best haze days and the worst haze days as selected using each algorithm and using the measured light scattering were examined. Table 6 contains the average composition by region of the country for days selected as best and worst by these three methods. The contributions to light extinction by the various components were not explicitly calculated, but are inherently somewhat different because of the explicit differences in the two algorithms. This table demonstrates that the new algorithm selects days with mean light scattering values that are somewhat closer to the mean values of measurement-selected best and worst days compared with the values using the original algorithm. It also indicates that the average composition associated with the best and worst haze days are not very sensitive to the method of identifying the sample periods for the best and worst categories.

Table 5. Percentage of days correctly classified by the original and revised algorithms as 20% best and 20% worst visibility days for sites east and west of the 100th meridian.

	20% Best Days (%)		20% Worst Days (%)	
Region	**Original**	**Revised**	**Original**	**Revised**
East	78	77	83	80
West	75	74	80	79

Table 6. Mean light scattering and percent PM_{10} composition for the major components on the 20% best and 20% worst haze days as selected by nephelometer measurements, the original algorithm, and the revised algorithm for sites east and west of the 100th meridian.

Region/ Extreme	Basis of Selection	Light Scattering (Mm^{-1})	Ammonium Sulfate (%)	Ammonium Nitrate (%)	Organic Mass (%)	Elemental Carbon (%)	Fine Soil (%)	Coarse Mass (%)
East/Best	Measured	10.7	22.9	4.7	20.7	2.8	4.1	44.6
	Original	14.0	22.4	5.0	21.3	3.0	4.0	44.2
	Revised	12.8	23.1	5.3	20.8	3.0	3.9	44.1
East/Worst	Measured	91.1	39.0	5.4	21.4	2.5	3.9	27.9
	Original	81.9	39.5	5.1	20.9	2.5	4.1	28.4
	Revised	90.8	39.5	4.4	21.6	2.5	3.8	28.7
West/Best	Measured	4.5	13.0	3.1	19.6	2.9	7.0	54.2
	Original	6.6	13.8	3.7	19.9	3.1	7.1	52.3
	Revised	5.9	14.1	4.0	19.6	3.3	6.9	52.0
West/Worst	Measured	36.0	16.6	5.2	26.5	2.8	7.5	41.3
	Original	32.2	16.2	5.2	25.1	2.6	7.6	43.5
	Revised	32.3	15.2	4.6	26.1	2.6	7.8	44.0

Similar results for each of the 21 nephelometer monitoring locations are available elsewhere.[31] Among the 21 sites, only Grand Canyon had any substantial variations in the composition between measurement-selected days compared with algorithm-selected days, both only involving nitrates and coarse mass. Grand Canyon nitrates and coarse mass contributed mean values of 16% and 50%, respectively, on the measurement-selected worst days, and 11% and 57%, respectively, for both algorithms selection of worst days, and measurement-selected best days for nitrate and coarse mass contributed mean values of 14% and 55%, respectively, compared with 18% and 48% for both algorithms-selected best days.

SUMMARY AND DISCUSSION

An algorithm to estimate light extinction at rural sites from IMPROVE network aerosol speciation data has been revised to reduce bias at the extremes and to incorporate more recent literature. The revised algorithm significantly reduces the biases compared with measurements at the high and low extremes. This is most apparent for sites in the hazier eastern United States. Compared with the original, the revised algorithm has marginally reduced precision (i.e., points on a scatter plot of estimated versus measured are further from the one-to-one line), with the result that there are somewhat (1–3%) more misclassified worst 20% haze days using the revised algorithm. However, the composition of days selected as best and worst by the original and the new algorithms are very similar, and similar to days selected by measurements.

Most of the reduction of bias associated with the new algorithm is attributed to the use of the split-component mass extinction efficiency method for sulfate, nitrate, and OC components that permitted variable mass extinction efficiency depending on the component mass concentration. Although not subject to explicit performance testing, the revised algorithm also contains specific changes from the original algorithm that reflect more recent scientific literature (e.g., change to 1.8 from 1.4 for OC mass to carbon mass ratio), a more complete accounting for contributors to haze (e.g. sea salt and NO_2 terms), and use of site-specific Rayleigh scattering to reduce elevation-related bias.

Both the original and revised algorithms were developed to enable consistent estimates of light extinction from IMPROVE aerosol data at remote area monitoring sites nationwide under the current range of aerosol conditions. These algorithms may not be appropriate for urban areas or for other substantially changed conditions. Regionally optimized and urban algorithms can be developed to better estimate light extinction (e.g., urban ratios of organic compound mass to carbon mass is lower than in remote areas). Most of the remote area monitoring sites do not have collocated RH or nephelometer data, so the algorithms are typically used with long-term monthly averaged water growth terms. For sites with collocated coincident RH, better light extinction estimates can be determined by using the day-specific RH data in the algorithm to account for particle water growth. Sites with collocated coincident nephelometer data can have site-optimized algorithms developed that would provide better estimates of light extinction than either the original or revised IMPROVE algorithms.

REFERENCES

1. van de Hulst, H.C. *Light Scattering by Small Particles*; Dover: New York, 1981.
2. McMeeking, G.R.; Kreidenweis, S.M.; Carrico, C.M.; Collett, J., Jr.; Day, D.E.; Malm, W.C. Observations of Smoke-Influenced Aerosol during the Yosemite Aerosol Characterization Study: 2. Aerosol Scattering and Absorbing Properties; *J. Geophys. Res.* **2005**, *110,* D18209, doi:10.1029/2004JD005624.
3. *Draft Guidance for Tracking Progress Under the Regional Haze Rule*; U.S. Environmental Protection Agency, Office of Air Quality Planning and Standards: Research Triangle Park, NC, September 27, 2001; available on U.S. Environmental Protection Web site at *http:/vista.cira.colostate.edu/improve/publications/guidancedocs/guidancedocs.htm* (accessed 2007).
4. Lowenthal, D.H.; Kumar, N. $PM_{2.5}$ Mass and Light Extinction Reconstruction in IMPROVE; *J. Air & Waste Manage. Assoc.* **2003**, *53,* 1109-1120.
5. Ryan, P.A.; Lowenthal, D.; Kumar, N. Improved Light Extinction Reconstruction in Interagency Monitoring of Protected Visual Environments; *J. Air & Waste Manage. Assoc.* **2005**, *55,* 1751-1759.
6. Hand, J.L.; Malm, W.C. *2005: Review of the IMPROVE Equation for Estimating Ambient Light Extinction Coefficients*; available on the IMPROVE Web site at *http://vista.cira.colostate.edu/improve/Publications/GrayLit/gray_literature.htm* (accessed 2007).
7. Sisler, J.F. *Spatial and Seasonal Patterns and Long Term Variability of the Composition of the Haze in the United States: an Analysis of Data from the IMPROVE Network*; CIRA Report to the National Park Service, ISSN: 0737-5352-32; available at *http://vista.cira.colostate.edu/improve/Publications/Reports/1996/1996.htm* (accessed 2007).
8. Lowenthal, D.H.; Kumar, N. Light Scattering from Sea Salt Aerosols at IMPROVE Sites; *J. Air & Waste Manage. Assoc.* **2006**, *56,* 636-642.

9. Pytkowicz, R.M.; Kester, D.R. The Physical Chemistry of Sea Water; *Oceanogr. Mar. Biol. Ann. Rev.* **1971**, *9,* 11-60.
10. McInnes, L.M.; Covert, D.S.; Quinn, P.K.; Germani, M.S. Measurements of Chloride Depletion and Sulfur Enrichment in Individual Sea-Salt Particles Collected from the Remote Marine Boundary Layer; *J. Geophys. Res.* **1994**, *99,* 8257-8268.
11. Quinn, P.K.; Marshall, S.F.; Bates, T.S.; Covert, D.S.; Kapustin, V.N. Comparison of Measured and Calculated Aerosol Properties Relevant to the Direct Radiative Forcing of Tropospheric Sulfate Aerosol on Climate; *J. Geophys. Res.* **1995**, *100,* 8977-8991.
12. Quinn, P.K.; Kapustin, V.N.; Bates, T.S.; Covert, D.S. Chemical and Optical Properties of Marine Boundary Layer Aerosol Particles of the Mid-Pacific in Relation to Sources and Meteorological Transport; *J. Geophys. Res.* **1996**, *101,* 6931-6951.
13. Quinn, P.K.; Coffman, D.J.; Kapustin, V.N.; Bates, T.S.; Covert, D.S. Aerosol Optical Properties in the Marine Boundary Layer During the First Aerosol Characterization Experiment (ACE 1) and the Underlying Chemical and Physical Aerosol Properties; *J. Geophys. Res.* **1998**, *103,* 16547-16563.
14. Tang, I.N.; Tridico, A.C.; Fung, K.H. Thermodynamic and Optical Properties of Sea Salt Aerosols; *J. Geophys. Res.* **1997**, *102,* 23269-23275.
15. Clegg, S.L.; Brimblecombe, P.; Wexler, A.S. A Thermodynamic Model of the System H^+-NH_4-Na^+-SO_4^{2-}-NO^{3-}-Cl^--H_2O at 298.15 K; *J. Phys. Chem.* **1998**, *102,* 2155-2171.
16. Grosjean, D.; Friedlander, S.K. Gas-Particle Distribution Factors for Organic and Other Pollutants in the Los Angeles Atmosphere; *J. Air Pollut. Control Assoc.* **1975**, *25,* 1038-1044.
17. White, W.H.; Roberts P.T. On the Nature and Origins of Visibility-Reducing Aerosols in the Los Angeles Air Basin; *Atmos. Environ.* **1977**, *11,* 803-812.
18. Andrews, E.; Saxena, P.; Musarra, S.; Hildemann, L.M.; Koutrakis, P.; McMurry, P.H.; Olmez, I.; White, W.H. Concentration and Composition of Atmospheric Aerosols from the 1995 SEAVS Experiment and a Review of the Closure between Chemical and Gravimetric Measurements; *J. Air & Waste Manage. Assoc.* **2000,** *50,* 648-664.
19. Turpin, B.J.; Lim, H.-J. Contributions to $PM_{2.5}$ Mass Concentrations: Revisiting Common Assumptions for Estimating Organic Mass; *Aerosol. Sci. Technol.* **2001**, *35,* 602-610.
20. Krivácsy, Z.; Gelencsér, A.; Kiss, G.; Mészáros, E.; Molnár, A.; Hoffer, A.; Mészáros, T.; Sárvári, Z.; Temesi, D.; Varga, B.; Baltensperger, U.; Nyeki, S.; Weingartner, E. Study on the Chemical Character of Water Soluble Organic Compounds in Fine Atmospheric Aerosol at the Jungfraujoch; *J. Atmos. Chem.* **2001**, *39,* 235-259.
21. Poirot, R.L.; Husar, R.B. Chemical and Physical Characteristics of Wood Smoke in the Northeastern U.S. during July 2002: Impacts from Quebec Forest Fires. Presented at the A&WMA Specialty Conference: Regional and Global Perspectives on Haze: Causes, Consequences and Controversies, Ashville, NC, October 25–29, 2004; Paper No. 94.
22. Malm, W.C.; Day, D.E.; Carrico, C.; Kreidenweis, S.M.; Collett, J.L., Jr.; McMeeking, G.; Lee; Carillo, J. Intercomparison and Closure Calculations Using Measurements of Aerosol Species and Optical Properties during the Yosemite Aerosol Characterization Study; *J. Geophys. Res.* **2005**, *110*, D14302, doi:10.1029/2004JD005494.
23. El-Zanan, H.S.; Lowenthal, D.H.; Zielinska, B.; Chow, J.C.; Kumar, N. Determination of the Organic Aerosol Mass to Organic Carbon Ratio in IMPROVE Samples; *Chemosphere* **2005**, *60,* 485-496.
24. Malm, W.C.; Hand, J.L. An Examination of the Physical and Optical Properties of Aerosols Collected in the IMPROVE Program; *Atmos. Environ.*, **2007**, *41*, 3404-3427.
25. Lowenthal, D.H.; Kumar, N. Variation of Mass Scattering Efficiencies in IMPROVE; *J. Air & Waste Manage. Assoc.* **2005**, *54*, 926-934.
26. Malm, W.C.; Day, D.E.; Kreidenweis, S.M.; Collett, J.L.; Lee, T. Humidity-Dependent Optical Properties of Fine Particles during the Big Bend Regional Aerosol and Visibility Study *J. Geophys. Res.* **2003,** *108,* 4279.
27. IMPROVE Web site; available at *http://vista.cira.colostate.edu/improve/*; VIEWS Web site; available at *http://vista.cira.colostate.edu/views/.*
28. Dixon, J.K. The Absorption Coefficient of Nitrogen Dioxide in the Visible Spectrum; *J. Chem. Phys.* **1940,** 8, 157-161.
29. *Draft Final Report: User's Manual For The Plume Visibility Model (PLUVUE)*; Systems Applications, Inc.: Alexandria, VA, July 1980.
30. *2-deg Color Matching Function*; CIE (1931); available on CVRL Color and Vision Database Web site at *http://www-cvrl.ucsd.edu/cmfs.htm* (accessed 2007).
31. *Revised IMPROVE Algorithm for Estimating Light Extinction from Particle Speciation Data*; Report to the IMPROVE Steering Committee; available at *http://vista.cira.colostate.edu/improve/publications/grayLit/019_revisedIMPROVEeq/revisedIMPROVEalgorithm3.doc* (accessed January 2006).

About the Authors

Marc Pitchford is a meteorologist with the National Oceanic and Atmospheric Administration, Las Vegas, NV. William Malm, a research physicist, and Bret Schichtel, a physical scientist, are with the National Park Service, Fort Collins, CO. Naresh Kumar is an area manager in air quality with the Electric Power Research Institute, Palo Alto, CA. Douglas Lowenthal is an associate research professor with the Desert Research Institute, Reno, NV. Jenny Hand is a research scientist with the Cooperative Institute Research in the Atmosphere, Colorado State University Fort Collins, CO. Please address correspondence to Marc Pitchford, National Oceanic and Atmospheric Administration, Air Research Laboratories, c/o Desert Research Institute, Las Vegas, NV 89119-7363; phone: +1-702-862-5432; fax: +1-702-862-5507; e-mail: marcp@dri.edu.